

A Continuous Rainfall Model based on Vine Copulas

Hilde Vernieuwe¹, Sander Vandenberghe², Bernard De Baets¹, and Niko E.C. Verhoest²

¹KERMIT, Department of Mathematical Modelling, Statistics and Bioinformatics, Ghent University, Coupure links 653, B-9000 Ghent, Belgium

²Laboratory of Hydrology and Water Management, Ghent University, Coupure links 653, B-9000 Ghent, Belgium

Correspondence to: Hilde Vernieuwe (hilde.vernieuwe@ugent.be)

Abstract. Copulas have already proven their flexibility in rainfall modelling. Yet, their use is generally restricted to the description of bivariate dependence. Recently, vine copulas have been introduced, allowing multi-dimensional dependence structures to be described on the basis of a stage by stage mixing of two-dimensional copulas. This paper explores the use of such vine copulas in order to incorporate all relevant dependences between the storm variables of interest. On the basis of such fitted vine copulas, an external storm structure is modeled. An internal storm structure is superimposed based on Huff curves, such that a continuous time series of rainfall is generated. The performance of the rainfall model is evaluated through a statistical comparison between an ensemble of synthetical rainfall series and the observed rainfall series and through the comparison of the annual maxima.

1 Introduction

Rainfall serves as an important base for many studies involving hydrological applications including flood risk estimation, the design of hydraulic structure and urban drainage systems or the evaluation of hydrological effects of climate change. Ideally, one should then have extensive observed rainfall time series at hand, both in time and space and at different time scales. Therefore, several rainfall modelling approaches have been proposed during the last decades (e.g. Kavvas and Delleur (1981); Rodriguez-Iturbe et al. (1987a, b); Katz and Parlange (1998); Menabde and Sivapalan (2000); Willems (2001); Evin and Favre (2008); Gyasi-Agyei (2011); Viglione et al. (2012)), which can be subdivided in models that generate design storms and models that allow for the simulation of continuous time series at a point or spatially distributed. Design storms are generally developed for a given return period and storm duration. The corresponding rainfall volume, obtained from e.g.

intensity-duration-frequency (IDF) curves is then assigned to the design storm according to a temporal rainfall pattern or internal storm structure (Chow et al., 1988). **However, this approach has an important drawback as it does not properly account for the antecedent wetness state of the catchment (Verhoest et al., 2010). Yet, this initial condition regulates the fractioning of the incident rainfall into runoff and infiltration and thus determines the fluvial response of a catchment to the imposed rainfall event. It was shown by Verhoest et al. (2010) that, because of this, the return period of the rainfall event may differ significantly from that of the corresponding discharge. In order to account for the antecedent soil moisture condition within the catchment, one can alternatively work with continuous rainfall models that provide input to rainfall-runoff models. As the latter models continuously update the soil moisture state, they therefore provide continuous estimates of the antecedent wetness state within the catchment.** Continuous rainfall models can be classified in four categories (Onof et al., 2000): (1) physically-based meteorological models; (2) stochastic multi-scale models that allow for modelling the spatial evolution of the rainfall process; (3) statistical models, preserving trends in precipitation and (4) stochastic process models that mimic the hierarchical structure of the rainfall process using a limited number of model parameters.

The variables that characterize a storm, *i.e.* the storm intensity, duration and volume, mostly exhibit some kind of mutual dependence: a long storm duration is more likely to be associated with a low storm intensity than with a high one. **It is therefore of utmost importance to construct joint probability distribution functions whenever frequency analysis studies, e.g. to analyse extremes, need to be carried out. Yet, the marginal probability distribution functions of these storm variables usually do not exhibit the same type of parametric distribution and are largely skewed (Vandenberghe et al., 2010b), *i.e.* there is a large deviation from the normal distribution. These characteristics hamper the identification of the joint probability distribution functions needed in order to calculate the probability of occurrence of a storm with a specific duration and intensity. The introduction of copulas in hydrology facilitated this task.**

Copulas are functions that couple the marginal distribution functions of the random variables into their joint distribution function and therefore describe the dependence structure between these random variables (Sklar, 1959). The great advantage of copulas is that the joint distribution function is built based on two independent tasks comprising the modelling of the dependence and the modelling of the marginal distribution functions. As this property allows for modelling a large variety of joint probability functions, copulas have been used within an increased number of publications in recent years. Pioneering work with respect to applying copulas in hydrology was performed by De Michele and Salvadori (2003); Salvadori and De Michele (2004); Favre et al. (2004) and De Michele et al. (2005). Concerning rainfall modelling, copulas offer a great flexibility in the modelling of high-dimensional dependence structures, however, determining parametric distributions for high-dimensional random vectors is complex (Aas and Berg, 2009). Copulas can, for in-

stance, improve many rainfall models that mimic the external rainfall process, *i.e.* the process of storm arrival, duration and mean intensity at the coarse scale (Salvadori and De Michele, 2007). These models mostly consider rainfall as a sequence of rectangular pulses, having a certain duration and mean intensity, followed by a specific dry period.

This paper explores how a point-scale rainfall model can be constructed using multivariate copulas, in order to incorporate all relevant dependences between the storm variables of interest. The application of multivariate copulas in hydrology is, in contrast to the application of bivariate copulas, a less explored domain. Some applications can be found in the modelling of trivariate rainfall (Zhang and Singh, 2007; Kao and Govindaraju, 2008; Salvadori and De Michele, 2006; Grimaldi and Serinaldi, 2006), trivariate floods (Serinaldi and Grimaldi, 2007; Genest et al., 2007; Ganguli and Reddy, 2013) and trivariate droughts (Song and Singh, 2010; Wong et al., 2010; Ma et al., 2013). Copula applications in hydrology that go beyond the trivariate case are still very scarce. One example is De Michele et al. (2007) who provide a study on constructing a copula for a four-dimensional sea storm phenomenon. The lack of successful applications of multivariate copulas in hydrology is, of course, influenced by the progress made in the theory of multivariate copulas. Due to the increase in dimensionality, the study of copulas becomes more complicated than in the bivariate case. Therefore, the question of how to construct a copula family that is sufficiently flexible to model the complete dependence structure is a very vivid one in theoretical research. Recently, a flexible construction method, based on mixing (conditional) bivariate copulas, has been introduced, which holds a large potential for many hydrological applications. In literature, this method is referred to as the vine-copula (or pair-copula) construction method (see e.g. Kurowicka and Cooke (2007); Aas et al. (2009); Aas and Berg (2009); Hobæk Haff et al. (2010)). The underlying theory for this method is given by Bedford and Cooke (2001, 2002) and stems from Joe (1997), which also forms the basis for the method of "conditional mixtures", as applied by De Michele et al. (2007). **The use of vine copulas is becoming popular in finance (see e.g. Nikololoupoulos et al. (2012); Zhang (2014); Mendes and Accioly (2014)) and geophysics and hydrology (see e.g. Gräler (2014); Xiong et al. (2014); Gyasi-Agyei and Melching (2012); Gräler et al. (2013)).**

The model that is developed in this paper consists of two submodels. In a first submodel, the vine-copulas-model, three- and four-dimensional vine copulas are used to describe the dependence between the storm duration, storm volume, the interstorm period following the storm and, in case a four-dimensional vine-copula is used, also the dry fraction within the storm. In a second submodel, the intrastorm-generating-model, the intrastorm variability is obtained based on Huff curves (Huff, 1967), **which plot the normalized cumulative storm depth against the normalized time since the beginning of a storm.** Before introducing the model, Section 2 provides some background on the construction of vine copulas and the simulation using vine copulas. Section 3 briefly introduces the historical time series, while Section 4 describes the rainfall model. In Section 5 the model per-

95 formance is assessed and a comparison with a state-of-the-art stochastic rainfall model is performed to further assess the performance of the newly introduced model.

2 Vine copulas

2.1 Construction

100 A vine copula mixes (conditional) bivariate copulas stage by stage in order to build a high-dimensional copula, i.e. the full density function is decomposed into a product of low-dimensional density functions. Consider the case of two random variables X and Y describing a phenomenon (e.g. storm duration and storm volume). Using their marginal distribution functions F_X and F_Y , the values of both random variables are transformed into values, respectively U and V , in the real unit interval $\mathbb{I} = [0, 1]$:

$$\begin{cases} u = F_X(x) \\ v = F_Y(y) \end{cases} \Leftrightarrow \begin{cases} x = F_X^{-1}(u) \\ y = F_Y^{-1}(v) \end{cases}, \quad (1)$$

105 where x, y, u and v are the values of the corresponding variables X, Y, U and V . U and V are uniformly distributed on \mathbb{I} . F_X^{-1} and F_Y^{-1} are the (quasi-)inverse functions of the distribution functions F_X and F_Y (Nelsen, 2006).

A bivariate copula or a 2-copula is a function $C : \mathbb{I} \times \mathbb{I} \rightarrow \mathbb{I}$ that satisfies:

1. for all $u, v \in \mathbb{I}$,

$$\begin{aligned} C(u, 0) = 0 \quad \text{and} \quad C(0, v) = 0 \\ C(u, 1) = u \quad \text{and} \quad C(1, v) = v \end{aligned} \quad (2)$$

110 2. for all $u_1, u_2, v_1, v_2 \in \mathbb{I}$ for which $u_1 \leq u_2$ and $v_1 \leq v_2$:

$$C(u_2, v_2) - C(u_2, v_1) - C(u_1, v_2) + C(u_1, v_1) \geq 0. \quad (3)$$

The extension of this definition to k dimensions results in a k -copula (see (Nelsen, 2006) for the definition and a detailed explanation). The theorem of Sklar (1959) relates bivariate copulas and bivariate distribution functions and states that for any two continuous random variables X_1 and X_2 , with continuous marginal cumulative distribution functions F_1 and F_2 , a unique bivariate copula 115 C_{12} exists such that

$$F_{12}(x_1, x_2) = C_{12}(F_1(x_1), F_2(x_2)) = C_{12}(u, v), \quad (4)$$

where F_{12} is the joint cumulative distribution function of X_1 and X_2 . This theorem thus formulates that a copula couples the marginal cumulative distribution functions of two random variables

into a joint cumulative distribution function F_{12} . This theorem can be extended to k dimensions and hence relates a k -dimensional cumulative distribution function $F_{12\dots k}$ to k marginal distribution functions (Sklar, 1959): for k continuous random variables X_1, X_2, \dots, X_k , with continuous marginal distributions functions F_1, F_2, \dots, F_k , there exists a unique k -copula $C_{12\dots k}$ such that:

$$F_{12\dots k}(x_1, x_2, \dots, x_k) = C_{12\dots k}(F_1(x_1), F_2(x_2), \dots, F_k(x_k)). \quad (5)$$

In order to explain the construction of vine copulas, the construction of a three-dimensional vine copula is first explained. The joint probability density function (PDF) f_{123} of a random vector (X_1, X_2, X_3) can, **for instance**, be decomposed as follows:

$$f_{123}(x_1, x_2, x_3) = f_{13|2}(x_1, x_3|x_2) \cdot f_2(x_2), \quad (6)$$

where $f_{13|2}$ is the joint PDF of X_1 and X_3 , given $X_2 = x_2$ and f_2 is the marginal PDF of X_2 . The joint cumulative distribution function (CDF) F_{123} is then obtained by integration, following the conditional mixtures approach (De Michele et al., 2007):

$$\begin{aligned} F_{123}(x_1, x_2, x_3) &= \int_{-\infty}^{x_1} \int_{-\infty}^{x_2} \int_{-\infty}^{x_3} f_{123}(r, s, t) dr ds dt \\ &= \int_{-\infty}^{x_1} \int_{-\infty}^{x_2} \int_{-\infty}^{x_3} f_{13|2}(r, t|s) f_2(s) dr ds dt \\ &= \int_{-\infty}^{x_2} \left[\int_{-\infty}^{x_1} \int_{-\infty}^{x_3} f_{13|2}(r, t|s) dr dt \right] f_2(s) ds \\ &= \int_{-\infty}^{x_2} F_{13|2}(x_1, x_3|s) dF_2(s) \\ &= \int_{-\infty}^{x_2} C_{13|2}(F_{1|2}(x_1|s), F_{3|2}(x_3|s)) dF_2(s). \end{aligned} \quad (7)$$

The conditional cumulative distribution functions $F_{1|2}(x_1|x_2)$ and $F_{3|2}(x_3|x_2)$ can also be expressed in terms of copulas:

$$\begin{aligned} F_{1|2}(x_1|x_2) &= \frac{\partial}{\partial u_2} C_{12}(u_1, u_2); \\ F_{3|2}(x_3|x_2) &= \frac{\partial}{\partial u_2} C_{23}(u_2, u_3), \end{aligned} \quad (8)$$

with $u_1 = F_1(x_1)$, $u_2 = F_2(x_2)$ and $u_3 = F_3(x_3)$. When instead of X_1, X_2 and X_3 , their transformed uniform random variables on \mathbb{I} , U_1, U_2 and U_3 , are considered, Eq. (7) can be expressed as follows:

$$C_{123} = \int_0^{u_2} C_{13|2} \left(\frac{\partial}{\partial s} C_{12}(u_1, s), \frac{\partial}{\partial s} C_{23}(s, u_3) \right) ds. \quad (9)$$

In the theory of vine copulas, the same decomposition of the density function is performed, but instead of using cumulative probability functions, all equations are rather expressed in terms of
140 density functions and the full density function c_{123} of the three-dimensional copula is then given by:

$$c_{123}(u_1, u_2, u_3) = c_{13|2}(F_{1|2}(x_1|x_2), F_{3|2}(x_3|x_2)) \cdot c_{12}(u_1, u_2) \cdot c_{23}(u_2, u_3). \quad (10)$$

Similarly, for a random vector (X_1, X_2, X_3, X_4) , the joint probability density function f_{1234} can, for instance, be decomposed as follows:

$$f_{1234}(x_1, x_2, x_3, x_4) = f_{14|23}(x_1, x_4|x_2, x_3) \cdot f_{23}(x_2, x_3). \quad (11)$$

145 The joint cumulative distribution function F_{1234} is then obtained by integration, similarly as in Eq. (7):

$$F_{1234}(x_1, x_2, x_3, x_4) = \int_{-\infty}^{x_2} \int_{-\infty}^{x_3} C_{14|23}(F_{1|23}(x_1|s, t), F_{4|23}(x_4|s, t)) dF_{23}(s, t). \quad (12)$$

Herein, the derivative of the bivariate CDF $F_{23}(x_2, x_3)$ is expressed as $dF_{23}(x_2, x_3) = f_{23}(x_2, x_3) dx_2 dx_3$. The functions $F_{1|23}(x_1|x_2, x_3)$ and $F_{4|23}(x_4|x_2, x_3)$ are con-
150 ditional cumulative distribution functions, and can also be expressed in terms of copulas:

$$F_{1|23}(x_1|x_2, x_3) = \frac{\partial C_{12|3}(F_{1|3}(x_1|x_3), F_{2|3}(x_2|x_3))}{\partial F_{2|3}(x_2|x_3)}, \quad (13)$$

$$F_{4|23}(x_4|x_2, x_3) = \frac{\partial C_{24|3}(F_{2|3}(x_2|x_3), F_{4|3}(x_4|x_3))}{\partial F_{2|3}(x_2|x_3)},$$

where the conditional CDFs $F_{1|3}$, $F_{2|3}$ and $F_{4|3}$ are calculated as in Eq. (8).

2.2 Fitting a three- or four-dimensional vine copula

Figures 1 and 2 illustrate the principle of constructing a three- respectively four-dimensional vine
155 copula. Consider tree 1 in Figures 1 and 2 where three (respectively four) uniform (on $[0, 1]$) random variables U_1, U_2 and U_3 (or U_1, U_2, U_3 and U_4) are given and their pairwise dependences are described by the bivariate copulas C_{12} and C_{23} (respectively C_{12}, C_{23} and C_{34}). Given a specific value of the second variable, these bivariate copulas can be conditioned (cfr. dashed arrows in Figures 1 and 2) through partial differentiation (Aas et al., 2009), resulting in the conditional cumulative distribution functions $F_{1|2}$ and $F_{3|2}$ (respectively $F_{1|2}, F_{3|2}, F_{2|3}$ and $F_{4|3}$). The pairwise dependences
160 between these conditional cumulative distribution functions are then captured by the bivariate copula $C_{13|2}$ (respectively the copulas $C_{13|2}$ and $C_{24|3}$). See tree 2 in Figures 1 and 2. These latter copulas can then also be conditioned by partial differentiation to obtain $F_{3|12}$ (respectively $F_{3|12}$ and $F_{4|23}$). For the four-dimensional vine copula, another bivariate copula $C_{14|23}$ captures the pairwise dependence between these conditional cumulative distribution functions and can on its turn be partially
165 differentiated to obtain $F_{4|123}$. See tree 3 in Figure 2. The conditional cumulative distribution functions $F_{3|12}$ and $F_{4|123}$ (of the three- and four-dimensional vine copula, respectively) will be of use

for simulation purposes (Aas et al., 2009). It should be noted that the hierarchical nesting of bivariate (conditional) copulas as presented here is just one of the possibilities and corresponds to what is called a D-vine (Aas et al., 2009).

In practice, the bivariate copulas in a higher tree of the vine copula (e.g. $C_{13|2}$) are fitted as follows. Consider a set of n data points, for all triplets $(u_{1,i}, u_{2,i}, u_{3,i})$ (or for all quadruplets $(u_{1,i}, u_{2,i}, u_{3,i}, u_{4,i})$), $i = 1, \dots, n$, the conditional CDF values (e.g. the CDF values according to $F_{1|2}$ and $F_{3|2}$ in the case of $C_{13|2}$) are calculated. The bivariate copulas (e.g. $C_{13|2}$) are then fitted to these ‘conditioned observations’, which are again approximately uniformly distributed on \mathbb{I} .

2.3 Generating samples out of the vine copula

A general simulation algorithm is presented next, borrowed from the theory on conditional mixtures. The literature on vine copulas reports very similar simulation algorithms (Aas and Berg, 2009; Aas et al., 2009). In order to simulate a random sample (u_1, u_2, u_3) (or (u_1, u_2, u_3, u_4)) out of the three- (or four-dimensional) conditional mixture copula, *i.e.* U_1, U_2, U_3 (and U_4) are uniformly distributed on \mathbb{I} , the one-dimensional conditional cumulative distribution function (CCDF) is highly important and is defined as (De Michele et al., 2007):

$$G_{k|1\dots k-1}(u_k|u_1, \dots, u_{k-1}) = \mathbb{P}(U_k \leq u_k | U_1 = u_1, \dots, U_{k-1} = u_{k-1})$$

$$= \frac{\frac{\partial^{k-1}}{\partial u_1 \dots \partial u_{k-1}} C_{1\dots k}(u_1, \dots, u_k)}{\frac{\partial^{k-1}}{\partial u_1 \dots \partial u_{k-1}} C_{1\dots k-1}(u_1, \dots, u_{k-1})}. \quad (14)$$

Herein, the numerator is the mixed partial derivative of the k -dimensional copula with respect to the conditioning variables. The denominator is the copula density of the $(k-1)$ -dimensional copula of the conditioning variables. In order to simulate a random sample out of the three- (respectively four-) dimensional conditional mixture copula, a random sample (t_1, t_2, t_3) (or (t_1, t_2, t_3, t_4)) should be first generated from (T_1, T_2, T_3) (respectively (T_1, T_2, T_3, T_4)) which are uniformly distributed random variables on \mathbb{I} , and serve as random probability levels of the CCDFs in the simulation algorithm which is listed next (of course for generating a three-dimensional sample, step 4 should not be performed):

1. $u_1 = t_1$;

2. $u_2 = G_{2|1}^{-1}(t_2|u_1)$, where

$$G_{2|1}(u_2|u_1) = \frac{\partial}{\partial u_1} C_{12}(u_1, u_2); \quad (15)$$

3. $u_3 = G_{3|12}^{-1}(t_3|u_1, u_2)$, where

$$G_{3|12}(u_3|u_1, u_2) = \frac{\frac{\partial^2}{\partial u_1 \partial u_2} C_{123}(u_1, u_2, u_3)}{\frac{\partial^2}{\partial u_1 \partial u_2} C_{12}(u_1, u_2)}; \quad (16)$$

4. $u_4 = G_{4|123}^{-1}(t_4|u_1, u_2, u_3)$, where

$$G_{4|123}(u_4|u_1, u_2, u_3) = \frac{\frac{\partial^3}{\partial u_1 \partial u_2 \partial u_3} C_{1234}(u_1, u_2, u_3, u_4)}{\frac{\partial^3}{\partial u_1 \partial u_2 \partial u_3} C_{123}(u_1, u_2, u_3)}. \quad (17)$$

The calculation of some partial derivatives, necessary for obtaining the CCDF $G_{4|123}$ is given below:

$$\begin{aligned} & \frac{\partial^3}{\partial u_1 \partial u_2 \partial u_3} C_{1234}(u_1, u_2, u_3, u_4) \\ 200 \quad &= \frac{\partial}{\partial u_1} C_{14|23}(G_{1|23}(u_1|u_2, u_3), G_{4|23}(u_4|u_2, u_3)), \end{aligned} \quad (18)$$

with

$$\begin{aligned} G_{1|23}(u_1|u_2, u_3) &= \frac{\frac{\partial^2}{\partial u_2 \partial u_3} C_{123}(u_1, u_2, u_3)}{\frac{\partial^2}{\partial u_2 \partial u_3} C_{23}(u_2, u_3)} \\ &= \frac{\frac{\partial}{\partial u_3} C_{13|2} \left(\frac{\partial}{\partial u_2} C_{12}(u_1, u_2), \frac{\partial}{\partial u_2} C_{23}(u_2, u_3) \right)}{\frac{\partial^2}{\partial u_2 \partial u_3} C_{23}(u_2, u_3)}, \end{aligned} \quad (19)$$

and

$$\begin{aligned} G_{4|23}(u_4|u_2, u_3) &= \frac{\frac{\partial^2}{\partial u_2 \partial u_3} C_{234}(u_2, u_3, u_4)}{\frac{\partial^2}{\partial u_2 \partial u_3} C_{23}(u_2, u_3)} \\ &= \frac{\frac{\partial}{\partial u_3} C_{24|3} \left(\frac{\partial}{\partial u_3} C_{23}(u_2, u_3), \frac{\partial}{\partial u_3} C_{34}(u_3, u_4) \right)}{\frac{\partial^2}{\partial u_2 \partial u_3} C_{23}(u_2, u_3)}. \end{aligned} \quad (20)$$

205 Once u_1, u_2, u_3 and u_4 are simulated, the corresponding values of x_1, x_2, x_3 and x_4 can be calculated by means of the inverse marginal cumulative distribution functions $F_1^{-1}, F_2^{-1}, F_3^{-1}$ and F_4^{-1} , respectively.

3 Historical time series characteristics

The time series used in this paper for fitting the model consists of a 105-year 10-minute rainfall
 210 record of Uccle, Belgium. These data were obtained by a Hellmann-Fuess pluviograph, installed in and operated by the Royal Meteorological Institute at Uccle near Brussels, Belgium (Demarée, 2003). This exceptional time series has been used in several studies, albeit with varying lengths, concerning statistical analyses (Vaes et al., 2002; De Jongh et al., 2006; Ntegeka and Willems, 2008; Vandenberghe et al., 2010b) and stochastic rainfall modelling (Verhoest et al., 1997; Vandenberghe et al.,
 215 2011; Vanhaute et al., 2012; Evin and Favre, 2013; Pham et al., 2013). For the current study, storms were first selected and their characteristics of interest calculated. Storms were selected on the basis of a minimal dry duration that separates two storms. Any dry period shorter than this threshold is thus considered to be part of a storm (Bonta and Rao, 1988). Similar to Verhoest et al. (1997) and Vandenberghe et al. (2010a, b); Vandenberghe et al. (2011), a dry period of 24 h was chosen,
 220 as this period assures that the arrival times of independent storms are Poisson distributed

(Restrepo-Posada and Eagleson, 1982). In this way, 8665 storms were selected and the following characteristics calculated: the onset of a storm (day, month, year), the storm volume V [mm], the storm duration W [h], the dry duration after the storm D [h], and the fraction dry within the storm p_d . It was observed that events with identical values of variables occur in the observed time series. As this is not desirable for a copula-based analysis, in which ranks are important, random noise, uniformly distributed between -0.1 mm and $+0.1$ mm was introduced to all strictly positive 10 minute observations as described and motivated in Vandenberghe et al. (2010b). The choice of 0.1 mm was based on the pluviograph's resolution. We also refer to Vandenberghe et al. (2010b) for a profound analysis of the dependences between the variables W , V , and D . Vandenberghe et al. (2010b) asserted that the hypothesis of stationarity of storms on the Uccle time series is fulfilled through seasonally subdividing the storms allowing copulas to be fitted per season. Therefore, the storm characteristics of the 105-year 10-minute rainfall time series are subdivided according to the season in which the storms occurred. To this end, similarly as in Vandenberghe et al. (2010b), winter is defined as the months December, January and February, spring as the months March, April and May, summer as the months June, July and August and autumn as the months September, October and November. It was furthermore noticed that some of the storms have no internal dry 10 minute intervals, *i.e.* $p_d = 0$. The set of storms within each season is then further subdivided into a subset of storms for which $p_d = 0$ and a subset of storms for which $p_d \neq 0$. The observed probability of $p_d = 0$ for the different seasons is listed in Table 1.

A kernel-smoothed distribution function was fitted to the observed values of W , V , D and p_d as none of the commonly used probability distributions fitted well the data. As D has a theoretical minimum of 24 h, due to the selection criterion, the distribution was fit to $D - 24$ h values, and afterwards, 24 h were added.

As the storm characteristics V , W and D do not reveal any information on the internal storm structure, and p_d only gives partial information, Huff curves, as derived in Vandenberghe et al. (2010a) are employed to provide statistical information on the internal structure. **The idea to use Huff curves to generate an internal storm structure has also been adopted by Candela et al. (2014).** Given the 105-year time series at hand, empirical Huff curves can be obtained by partitioning each storm in the time series in e.g. 20 identical time intervals at every 5% of the total storm duration. Furthermore, storms were classified into seasons, and quartile groups according to the **quarter** of the storm **duration** that received the largest amount of rainfall. For each season and each quartile group the corresponding Huff curves were obtained by visualizing the 10% and 90% percentiles of the distribution. In this way, 16 Huff curves were obtained (four quartile groups per season). As an example, Figure 3 illustrates the 10% and 90% percentile curves of the second quartile autumn storms. Vandenberghe et al. (2010a) showed that these curves are independent of the extremity of the storm.

4 Description of the rainfall model

4.1 The vine-copulas-submodel: Construction and use of vine copulas in the generation of a time series

By examining the storm characteristics of the historical time series, it is observed that some storms
260 have internal dry 10 minute intervals while others have not. It was decided to fit, for each season, a
four-dimensional vine copula to the values of W , V , D and the non-zero values of p_d . Furthermore,
for each season, a three-dimensional vine copula was fitted to the values of W , V and D in case
 $p_d = 0$. In this way, dependences between the variables for $p_d = 0$ and $p_d \neq 0$ are taken into account
and four three-dimensional and four four-dimensional vine copulas are obtained.

265 **The ordering of the copulas in the vine copula, *i.e.* the selection of a D-vine, is based on the
values of Kendall's tau as listed in Table 2. These values show that the strongest dependences
exist between the variables W and V , p_d and W , and V and D . By putting the most dependent
pair of variables in the first tree of the vine copula, the structure of a D-vine is established.**

The three- (W , V , and D) and four-dimensional (p_d, W , V , D) vine copulas are fitted stage by
270 stage, following the method explained in Section 2.2. We are aware that different copula families
could be used to describe the dependences between the different variables (cfr. Vandenberghe et al.
(2010b)). Yet, in this **conceptual** study, we opted to restrict to the Frank copula family to describe
the (conditional) bivariate dependences within the vine copulas, because of its ability to represent
positive or negative dependence. Furthermore, this family is frequently applied to describe bivariate
275 hydrological phenomena (Pan et al., 2013). Alternative families could better fit the different depen-
dences within the vine copula, however, the search for the best fitting copula was out of the scope
of the current study. It should be remarked that two different ways of parameterizing the Frank cop-
ula exist. In this paper, the one that has the dependence parameter range of $[-\infty, +\infty]$ is employed.

**The parameters of the Frank copulas are numerically estimated using the relationship between
280 Kendall's tau and the parameter value of the Frank copula (Genest, 1987):**

$$\tau_K = 1 - \frac{4}{\theta} \left(1 - \frac{1}{\theta} \int_0^\theta \frac{t}{e^t - 1} dt \right), \quad (21)$$

The fitted Frank copula parameters are presented in Table 3. **Figures 4 and 5 show the contours
of the Frank copulas and the empirical copulas for the three- and four-dimensional vine cop-
ula for the first season. It can be seen that the Frank copula fits the empirical copulas fairly
285 well. Only the dependence between W and V in the three-dimensional vine copula and the de-
pendence between p_d and W , and $W|V$ and $D|V$ in the four-dimensional vine copula are less
well represented. In order to check whether the vine copulas preserve the dependence between
the variables, two samples, with size 10 000, are simulated using the three- and four-dimensional
vine copulas, respectively, based on the method described in Section 2.3. Table 2 shows the good
290 correspondence between the observed and simulated pairwise dependences. To be able to transform**

samples from the fitted copula to real samples, the (inverse) marginal cumulative distribution functions of p_d , W , V and D are employed.

The inverse CDFs are then used to transform simulated uniformly distributed values in \mathbb{I} to values in \mathbb{R} . Once the simulated values of the quadruplet (p_d, W, V, D) are known, a time series of 105 years of rectangular rainfall pulses with duration W and height $I = V/W$, being separated by a dry duration D , is obtained. Of course, these rectangular pulses only correspond to the external storm structure. At this stage, only the timing of the beginning and the end of a storm is important. The pulse itself, characterized by W , V and p_d , needs to be further disaggregated into finer scale rainfall, which is elaborated upon in the next section.

300 4.2 The intrastorm-generating-submodel: Disaggregation of rectangular pulses by means of Huff curves

In order to employ Huff curves in the disaggregation of the rectangular pulses, a random quartile group is first assigned based on the probabilities of occurrence of the four quartile groups, as indicated in Table 4. By assigning the first pulse of the generated time series to the beginning of the year, the season of each simulated pulse is easily derived. On the basis of the probability of $p_d = 0$, the three- or four-dimensional vine copula for the corresponding season is employed to obtain simulated storm pulses. Next, as the season and the quartile group are known, a random internal storm structure can be assigned to each simulated storm pulse on the basis of the corresponding 10% and 90% Huff curves. To this end, time **instants** corresponding to the end of each 10 minute interval within the storm are selected. The 10% and 90% curves are then interpolated such that the values of the normalized cumulative storm depth for each of these time **instants** (expressed as a percentage of the total storm duration) are obtained.

The internal storm structure is then generated as follows. Firstly, time intervals having zero rainfall are randomly assigned within the storm such that the sampled value of p_d is respected. **It should be noted that the first and the last interval of the storm cannot have zero rainfall in order to preserve the duration W of the storm. Furthermore, when the value of p_d is such that the storm should only contain one wet 10 minute interval (i.e. p_d is close to one), the rainfall depth is evenly divided among the first and last 10 minute intervals. In addition**, the total length of a dry spell within a storm is constrained to 23 hours, i.e. one hour less than the selection criterion, in order to avoid that one storm would result in two different storms when the same storm selection criterion is applied on the simulated rainfall series. **It should also be mentioned that** storms that have a duration smaller than 40 minutes and for which $p_d \neq 0$, are disregarded in the generation of the rainfall series, because of the inability to assure the generation of the imposed quartile storm.

Secondly, the cumulative storm depths are randomly selected. This procedure calculates the normalized cumulative depth at the end of a time interval, i.e. at time instant b , before moving to

the next time interval. During the generation of the internal storm structure, three cases may occur, requiring different sampling strategies. These cases are:

1. Time **instant** b is situated in between two consecutive wet 10 minute intervals. In this case, a cumulative storm depth is randomly selected between the 10% and the 90% percentile curves, ensuring that the cumulative storm depths do not decrease in time. Figure 6(a) illustrates this **instant**, where time **instant** a denotes the previous time **instant** at which a value $D_{nc}(a)$ was selected, with D_{nc} **the normalized cumulative storm depth**. The current time **instant** b , at which a value $D_{nc}(b)$ is to be selected, is also indicated. $D_{nc}(b)$ **is randomly selected between a minimal ($H_{10}(b)$) and a maximal value ($H_{90}(b)$)**, indicated in the figure. $H_{10}(b)$, **respectively $H_{90}(b)$, denote the value of the 10%, respectively 90% Huff curve, at instant b .**
2. Time **instant** b corresponds to the end of a dry period. In this case, depicted in Figure 6(b), no sampling has to be performed (as the time interval between a and b should be dry), and thus the cumulative storm depth takes the value of the previous time **instant**, *i.e.* $D_{nc}(b) = D_{nc}(a)$, where $D_{nc}(b)$ may be situated outside the percentile curves.
3. Time **instant** b corresponds to the end of a wet period. In **this** third case, depicted in Figures 6(c) and (d), **the dry period starts at time instant b and ends at time instant c** . Two sampling strategies are possible, **among which is chosen with equal probability**. It is allowed that a cumulative storm depth is **sampled according to the 10% and 90% Huff curves either at time instant b or at time instant c** . When the first strategy is chosen (*cf.* Figure 6(c)), $D_{nc}(b)$ is sampled from the interval $[\max(D_{nc}(a), H_{10}(b)), H_{90}(b)]$, and the sampled value can hence be smaller **than $H_{10}(c)$, which indicates that the generated Huff curve will intersect the 10% Huff curve, before reaching time instant c and will hence not remain between the 10 and 90% boundaries. When the second strategy is chosen (*cf.* Figure 6(d)), $D_{nc}(b)$ is drawn from $[\max(D_{nc}(a), H_{10}(c)), H_{90}(c)]$, **i.e. the sample is chosen according to the 10% and 90% Huff curves at time instant c . The sampled value can hence be larger than $H_{90}(b)$, which indicates that the generated Huff curve will intersect the 90% Huff curve before reaching time instant b** . Such flexibility is required as the fraction of dry spells often does not allow to remain between the 10 and 90% boundaries. However, this flexibility is not a major problem, as **at each time interval within the storm** there are always 20% of the historical relative cumulative storm depths outside these boundaries by definition.**

Based on the historical time series, it was observed that the increment in cumulative storm depth between two subsequent time **instants** in a Huff curve is not uniformly distributed (this observation was neglected in Vandenberghe et al. (2010a)). Smaller increments occur more often than large increments. This behaviour is simulated by first establishing a cumulative probability distribution of strictly positive increments on the basis of the 105-year time series. To this end, for all storms in

a particular season and quartile group, the frequencies of normalized (strictly positive) increments of cumulative rainfall depths between two subsequent wet periods were recorded. This empirical cumulative distribution function for the respective season and quartile group is then used to randomly select a normalized **increase in** storm depth for the subsequent wet time **interval**. Figure 7 illustrates the use of the cumulative distribution in the sampling procedure. In this figure, the minimum and maximum bounds of the increments are first determined on the basis of the Huff curves, as explained above. These bounds are then transferred to the cumulative distribution of normalized increments between which a value is randomly selected by uniformly sampling within **this** sampling range (*cf*: Figure 7). **The corresponding difference percentage of total storm depth is then obtained.**

5 Results

It is common to validate the performance of a model through comparing statistics of one modeled time series to those calculated on the observed time series. However, given that the model has a stochastic nature, the statistics of the simulated time series will show some variability. To account for these stochastic effects, the model described in the previous section is employed to generate an ensemble of 100 time series of 105 years of 10-minute rainfall (*i.e.* similar to the length of the observed time series). In order to evaluate whether the model performs well in the reproduction of aggregated rainfall statistics, the 100 time series are furthermore regarded as equally probable realisations and the statistics are calculated on a yearly basis. The traditional first and second order statistical moments (*i.e.* mean and variance), autocorrelation (AC) at different time lags and the zero depth probability (ZDP) are calculated along with the third order central moment (skewness). These statistics are calculated on a yearly basis for each ensemble member at aggregation levels of 1/6, 1, 3, 6, 12 and 24 hours. Thus, for an aggregation level, 100×105 values of each of these statistics are obtained, such that a bundle of 100 empirical cumulative distributions can be established, *i.e.* one distribution per ensemble member. The empirical cumulative distribution of the values of the statistics of the observed time series can then be compared with this bundle. If the empirical cumulative distribution function of the observed statistics is situated within the bundle of distributions obtained by the model, the model performs well.

Figure 8(a) visualises the bundles of the 100 empirical cumulative distributions of the yearly statistics of the time series generated by the copula-based model and the empirical cumulative distribution of the yearly statistics of the observed time series for a 10-min aggregation level. Figure 8(b) displays the comparison for a 1-h aggregation level. These figures show that the observed mean is well represented by the copula-based model. For a 10-min aggregation level, also the ZDP is fairly well represented. The variance and the third central moment are overestimated, whereas the lag-1 and lag-2 autocovariances are underestimated. For the 1-h aggregation level, the ZDP and the lag-

1 autocovariance are underestimated, the other statistics are fairly well represented. For the other aggregation levels, only the mean is well represented. The other statistics are sometimes well represented, under- or overestimated. **With respect to** the ZDP-statistic, the fact that this statistic is well
400 **represented** at a 10-min aggregation level, yet, underestimated at higher aggregation levels (except for a 24-h aggregation level), is probably due to the selection of the dry periods within the storm. For storms that have a duration of more than one hour, these zero intervals are probably not connected as no temporal correlation is taken into account during the selection of dry periods, such that less dry periods are obtained after the aggregation than what is observed in the Uccle time series. Future
405 research will further elaborate on a better selection of dry periods within the storm.

As simulated time series are often used to simulate extreme discharges (Verhoest et al., 2010), the behaviour of the modelled extreme rainfall was also assessed. Figure 9 shows the annual maximum rainfall depths of the ensemble and of the observed rainfall series related to empirical return periods, considering six different aggregation levels. This figure shows that the extrema are well modelled
410 albeit the model overestimates extremes at short aggregation levels and tends to underestimate extremes at larger aggregation levels. Notwithstanding the shortcomings highlighted, this novel modelling concept **holds promise**. It should furthermore be stressed that other stochastic models such as the state-of-the-art Bartlett-Lewis models also are not able to preserve all statistics.

6 Conclusions

415 This study is the first in its kind in which a continuous stochastic rainfall generator is developed that uses vine copulas to describe the storms and their arrival process. The internal storm structure is based on the concept of Huff curves, while the fraction of dry periods within the storm is determined by the copulas. The main advantage of this approach is that the model is completely data driven and is **easier to calibrate than other rainfall generators such as the commonly used Modified**
420 **Bartlett Lewis model as, once the structure of the vine copula is determined, the calibration is reduced to estimating the parameters of the bivariate copulas. It should, however, be noted that we have at our disposal an exceptionally long time series of rainfall data on the basis of which the vine copulas are determined. If one would follow the same approach and search for the best-fitting copula family on a more commonly shorter time series of e.g. < 50 years**
425 **of rainfall data, one could be faced with difficulties as the number of storms per season may become too small for fitting the copulas.**

The model applies three- and four-dimensional vine copulas to describe the dependence between the different storm characteristics. The three-dimensional vine copulas are employed to describe the
430 seasonal dependence between storm duration, storm volume, and the interstorm period for storms that have no dry fraction within the storm. The four-dimensional vine copulas are employed to de-

scribe the seasonal dependence between these storm characteristics and the dry fraction within the storm. These vine copulas were fitted to the observed storm characteristics of a 105-years time series of 10-minute rainfall. Because of its frequent successful application in hydrological applications, 435 the Frank copula family was chosen to be used within the vine copulas. On the basis of these vine copulas, values of these four storm characteristics were drawn, representing the external storm structure, ensuring a time series of 105 year of rectangular rainfall pulses. According to their seasonal probability of occurrence, storms with zero dry fractions were sampled from the three-dimensional vine copulas. The internal storm structure of the rectangular pulses is superimposed based on Huff 440 curves, which were identified on the basis of the observed time series, leading to the generation of continuous 10-minute rainfall time series. In the generation of the internal storm structure, it is ensured that the fraction of dry periods within the storm as drawn from the vine copulas, is maintained. The internal storm structures are furthermore generated according to the probability of occurrence of the quartile storms in the observed time series, and the season in which they occur. In order to 445 determine the difference of cumulative storm depths in the internal storm structure, the empirical cumulative probability distribution function of increments between two subsequent wet periods in the storm is employed. In this way it is guaranteed that smaller increments occur more often than larger increments, as was observed in the measured time series.

In order to evaluate the performance of the rainfall model, an ensemble of 100 time series of 450 *ca.* 105 year 10-minute rainfall was generated, such that stochastic effects were accounted for. The results show that the copula-based rainfall model represents the mean value of the time series well, whereas the other statistics are either represented (fairly) well, over- or underestimated, depending on the aggregation level. A second evaluation of the generated ensemble encompassed the calculation of the annual maximum series, for different aggregation levels. It was observed that the annual 455 maxima simulated by means of the copula-based model were larger than the observed maxima for an aggregation level of 10 min, and the moderate return period of the 24-h aggregation level. For aggregation levels of 1 h – 12 h and the smaller and larger return periods of an aggregation level of 24 h, a good correspondence between the simulated and observed extremes was observed. Future research will reveal whether the representation of the ZDP-statistic for larger aggregation levels by 460 the copula-based model can be improved by better selecting the internal dry storm periods. The performance of the copula-based model will also be compared to state-of-the-art stochastic rainfall generators. **Also, it should be investigated whether including other bivariate copula families in the vine copulas can further improve the performance of the vine-copula-based model.**

Acknowledgements. This research has been performed in the framework of projects G.0837.10 and G.0013.11 465 granted by the Research Foundation Flanders.

References

- Aas, K. and Berg, D.: Models for construction of multivariate dependence - a comparison study, *European Journal of Finance*, 15, 639–659, 2009.
- Aas, K., Czado, C., Frigessi, A., and Bakken, H.: Pair-copula constructions of multiple dependence, *Insurance: Mathematics and Economics*, 44, 182–198, 2009.
- 470 Bedford, T. and Cooke, R.: Probability density decomposition for conditionally dependent random variables modeled by vines, *Annals of Mathematics and Artificial Intelligence*, 32, 245–268, 2001.
- Bedford, T. and Cooke, R.: Vines - A new graphical model for dependent random variables, *Annals of Statistics*, 30, 1031–1068, 2002.
- 475 Bonta, J. and Rao, A.: Factors affecting the identification of independent storm events, *Journal of Hydrology*, 98, 275–293, 1988.
- Candela, A., Brigandi, G., and Aronica, G.: Estimation of synthetic flood design hydrographs using a distributed rainfall-runoff model coupled with a copula-based single storm rainfall generator, *Natural Hazards and Earth System Sciences*, 14, 1819–1833, 2014.
- 480 Chow, V., Maidment, D., and Mays, L.: *Applied Hydrology*, McGraw-Hill Book Company, New York, 1988.
- De Jongh, I., Verhoest, N., and De Troch, F.: Analysis of a 105-year time series of precipitation observed at Uccle, Belgium, *International Journal of Climatology*, 26, 2023–2039, 2006.
- De Michele, C. and Salvadori, G.: A generalized Pareto intensity-duration model of storm rainfall exploiting 2-copulas, *Journal of Geophysical Research*, 108, 2003.
- 485 De Michele, C., Salvadori, G., Canossi, M., Petaccia, A., and Rosso, R.: Bivariate statistical approach to check adequacy of dam spillway, *Journal of Hydrologic Engineering*, 10, 50–57, 2005.
- De Michele, C., Salvadori, G., Passoni, G., and Vezzoli, R.: A multivariate model of sea storms using copulas, *Coastal Engineering*, 54, 734–751, 2007.
- Demarée, G.: The centennial recording raingauge of the Uccle Plateau: Its history, its data and its applications, *La Houille Blanche - Revue Internationale de l'Eau*, 4, 95–102, 2003.
- 490 Evin, G. and Favre, A.-C.: A new rainfall model based on the Neyman-Scott process using cubic copulas, *Water Resources Research*, 44, W03 433, 2008.
- Evin, G. and Favre, A.-C.: Further developments of a transient Poisson-cluster model for rainfall, *Stochastic Environmental Research and Risk Assessment*, 27, 831–847, 2013.
- 495 Favre, A., Adlouni, S. E., Perreault, L., Thiémondge, N., and Bobee, B.: Multivariate hydrological frequency analysis using copulas, *Water Resources Research*, 40, W01 101, 2004.
- Ganguli, P. and Reddy, M.: Probabilistic assessment of flood risks using trivariate copulas, *Theoretical and Applied Climatology*, 111, 341–360, 2013.
- Genest, C.: Frank's family of bivariate distributions, *Biometrika*, 74, 549–555, 1987.
- 500 Genest, C., Favre, A., Beliveau, J., and Jacques, C.: Metaelliptical copulas and their use in frequency analysis of multivariate hydrological data, *Water Resources Research*, 43, W09 401, 2007.
- Gräler, B.: Modelling skewed spatial random fields through the spatial vine copula, *Spatial Statistics*, 10, 87–102, 2014.

- Gräler, B., van den Berg, M., Vandenberghe, S., Petroselli, A., Grimaldi, S., De Baets, B., and Verhoest, N.:
505 Multivariate return periods in hydrology: a critical and practical review focusing on synthetic design hydro-
graph estimation, *Hydrology and Earth System Sciences*, 17, 1281–1296, 2013.
- Grimaldi, S. and Serinaldi, F.: Design hyetograph analysis with 3-copula function, *Hydrological Sciences Journal*, 51, 223–238, 2006.
- Gyasi-Agyei, Y.: Copula-based daily rainfall disaggregation model, *Water Resources Research*, 47, W07 535,
510 2011.
- Gyasi-Agyei, Y. and Melching, C.: Modelling the dependence and internal structure of storm events for continuous rainfall simulation, *Journal of Hydrology*, 464, 249–261, 2012.
- Hobæk Haff, I., Aas, K., and Frigessi, A.: On the simplified pair-copula construction - Simply useful or too simplistic?, *Journal of Multivariate Analysis*, 101, 1296–1310, 2010.
- 515 Huff, F.: Time distribution of rainfall in heavy storms, *Water Resources Research*, 3, 1007–1019, 1967.
- Joe, H.: *Multivariate Models and Dependence Concepts*, Chapman and Hall, 1997.
- Kao, S. and Govindaraju, R.: Trivariate statistical analysis of extreme rainfall events via the Plackett family of copulas, *Water Resources Research*, 44, 2008.
- Katz, R. and Parlange, M.: Overdispersion phenomenon in stochastic modeling of precipitation, *Journal of*
520 *Climate*, 11, 591–601, 1998.
- Kavvas, M. and Delleur, J.: A stochastic cluster model of daily rainfall sequences, *Water Resources Research*, 17, 1151–1160, 1981.
- Kurowicka, D. and Cooke, R.: Sampling algorithms for generating joint uniform distributions using the vine-copula method, *Computational Statistics and Data Analysis*, 51, 2889–2906, 2007.
- 525 Ma, M., Song, S., Ren, L., Jiand, S., and Song, J.: Multivariate drought characteristics using trivariate Gaussian and Student t copulas, *Hydrological Processes*, 27, 1175–1190, 2013.
- Menabde, M. and Sivapalan, M.: Modeling of rainfall time series and extremes using bounded random cascades and Levy-stable distributions, *Water Resources Research*, 36, 3293–3300, 2000.
- Mendes, B. and Accioly, V.: Robust Pair-Copula based forecasts of realized volatility, *Applied Stochastic*
530 *Models in Business and Industry*, 30, 183–199, 2014.
- Nelsen, R.: *An Introduction to Copulas*, in: *Lecture Notes in Statistics*, edited by Bickel, P., Diggle, P., Fienberg, S., Krickeberg, K., Olking, I., Wermuth, N., and Zeger, S., p. 216, Springer-Verlag, New York, 2006.
- Nikololopoulos, A., Joe, H., and Li, H.: Vine copulas with asymmetric tail dependence and applications to financial return data, *Computational Statistics and Data Analysis*, 56, 3659–3673, 2012.
- 535 Ntegeka, V. and Willems, P.: Trends and multidecadal oscillations in rainfall extremes, based on a more than 100-year time series of 10 min rainfall intensities at Uccle, Belgium, *Water Resources Research*, 44, W07 402, 2008.
- Onof, C., Chandler, R., Kakou, A., Northrop, P., Wheeler, H., and Isham, V.: Rainfall modelling using Poisson-cluster processes: a review of developments., *Stochastic Environmental Research and Risk Assessment*, 14, 384–411, 2000.
540
- Pan, M., Yuan, X., and Wood, E. F.: A probabilistic view on drought recovery., *Geophys. Res. Lett.*, 40, 3637–3642, 2013.

- Pham, M., Vanhaute, W., Vandenberghe, S., De Baets, B., and Verhoest, N.: An assessment of the ability of Bartlett-Lewis type of rainfall models to reproduce drought statistics, *Hydrology and Earth System Sciences*, 17, 5167–5183, 2013.
- Restrepo-Posada, P. and Eagleson, P.: Identification of independent rainstorms, *Journal of Hydrology*, 55, 303–319, 1982.
- Rodriguez-Iturbe, I., Cox, D., and Isham, V.: Some models for rainfall based on stochastic point processes, *Proceedings of the Royal Society of London A*, 410, 269–288, 1987a.
- Rodriguez-Iturbe, I., Febres de Power, B., and Valdés, J.: Rectangular pulses point process models for rainfall: analysis of empirical data, *Journal of Geophysical Research*, 92, 9645–9656, 1987b.
- Salvadori, G. and De Michele, C.: Analytical calculation of storm volume statistics involving Pareto-like intensity-duration marginals, *Geophysical Research Letters*, 31, 2004.
- Salvadori, G. and De Michele, C.: Statistical characterization of temporal structure of storms, *Advances in Water Resources*, 29, 827–842, 2006.
- Salvadori, G. and De Michele, C.: On the use of copulas in hydrology: theory and practice, *Journal of Hydrologic Engineering*, 12, 369–380, 2007.
- Serinaldi, F. and Grimaldi, S.: Fully nested 3-copula: procedure and application on hydrological data, *Journal of Hydrologic Engineering*, 12, 420–430, 2007.
- Sklar, A.: Fonctions de répartition à n dimensions et leurs marges., *Publications de l’Institut de Statistique de l’Université de Paris*, 8, 229–231, 1959.
- Song, S. and Singh, V.: Meta-elliptical copulas for drought frequency analysis of periodic hydrologic data, *Stochastic Environmental Research and Risk Assessment*, 24, 425–444, 2010.
- Vaes, G., Willems, P., and Berlamont, J.: 100 years of Belgian rainfall: Are there trends?, *Water Science and Technology*, 45, 55–61, 2002.
- Vandenberghe, S., Verhoest, N., Buysse, E., and De Baets, B.: A stochastic design rainfall generator based on copulas and mass curves, *Hydrology and Earth System Sciences*, 14, 2429–2442, 2010a.
- Vandenberghe, S., Verhoest, N., and De Baets, B.: Fitting bivariate copulas to the dependence structure between storm characteristics: A detailed analysis based on 105 year 10 min rainfall, *Water Resources Research*, 46, W01 512, 2010b.
- Vandenberghe, S., Verhoest, N., Onof, C., and Baets, B. D.: A comparative copula-based bivariate frequency analysis of observed and simulated storm events: a case study on Bartlett-Lewis modeled rainfall, *Water Resources Research*, 47, W07 529, 2011.
- Vanhaute, W., Vandenberghe, S., Scheerlinck, K., De Baets, B., and Verhoest, N.: Calibration of the modified Bartlett-Lewis model using global optimization techniques and alternative objective functions, *Hydrology and Earth System Sciences*, 16, 873–891, 2012.
- Verhoest, N., Troch, P., and Troch, F. D.: On the applicability of Bartlett-Lewis rectangular pulses models in the modeling of design storms at a point, *Journal of Hydrology*, 202, 108–120, 1997.
- Verhoest, N., Vandenberghe, S., Cabus, P., Onof, C., Meca-Figueras, T., and Jameleddine, S.: Are stochastic point rainfall models able to preserve extreme flood statistics?, *Hydrological Processes*, 24, 3439–2445, 2010.

- Viglione, A., Castellarin, A., Rogger, M., Merz, R., and Blöschl, G.: Extreme rainstorms: Comparing regional envelope curves to stochastically generated events, *Water Resources Research*, 48, 2012.
- Willems, P.: A spatial rainfall generator for small spatial scales, *Journal of Hydrology*, 252, 126–144, 2001.
- 585 Wong, G., Lambert, M., Leonard, M., and Metcalfe, A.: Drought Analysis using trivariate copulas conditional on climatic states, *Journal of Hydrologic Engineering*, 15, 129–141, 2010.
- Xiong, L., Yu, K., and Gottschalk, L.: Estimation of the distribution of annual runoff from climatic variables using copulas, *Water Resources Research*, 50, 7134–7152, 2014.
- Zhang, D.: Vine copulas and applications to the European Union sovereign debt analysis, *International Review of Financial Analysis*, 36, 46–56, 2014.
- 590 Zhang, L. and Singh, V.: Gumbel-Hougaard copula for trivariate rainfall frequency analysis, *Journal of Hydrologic Engineering*, 12, 409–419, 2007.

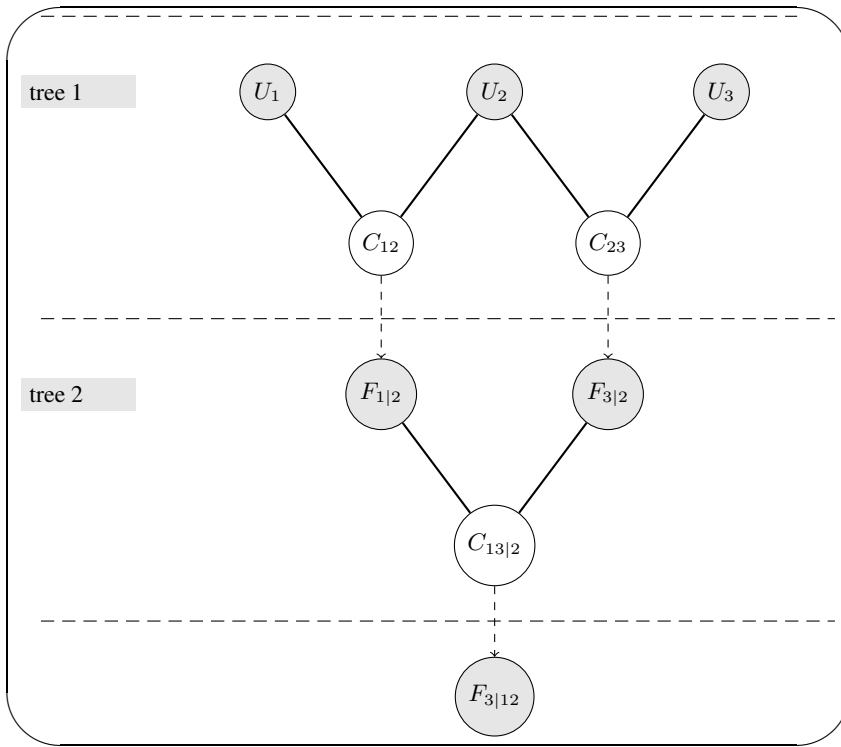


Figure 1. Hierarchical nesting of bivariate copulas in the construction of a three-dimensional vine copula through conditional mixtures.

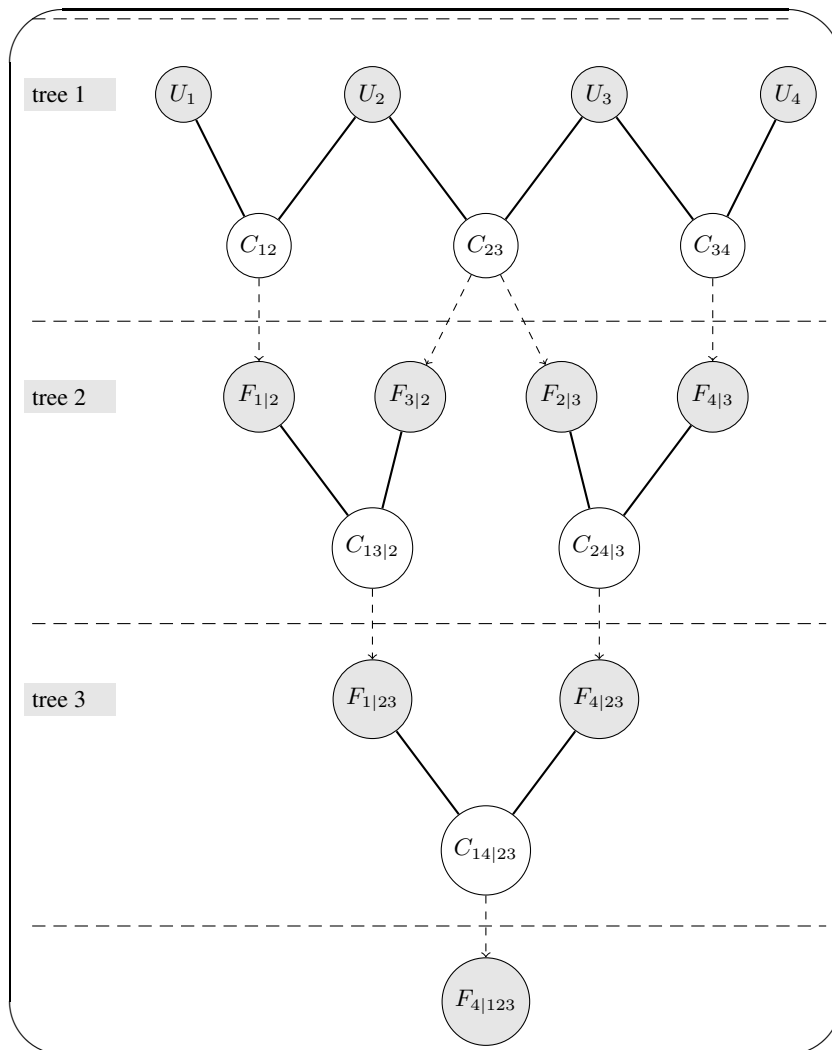


Figure 2. Hierarchical nesting of bivariate copulas in the construction of a four-dimensional vine copula through conditional mixtures.

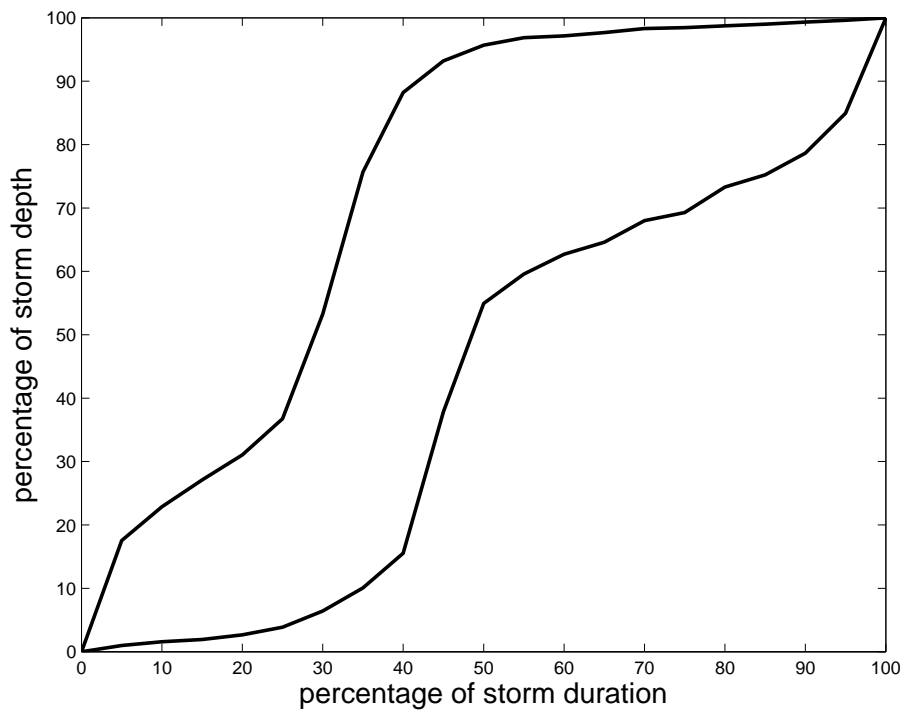


Figure 3. Huff curves for the second quartile autumn storms. The 10% (**lower**) and 90% (**upper**) percentile curves are given.

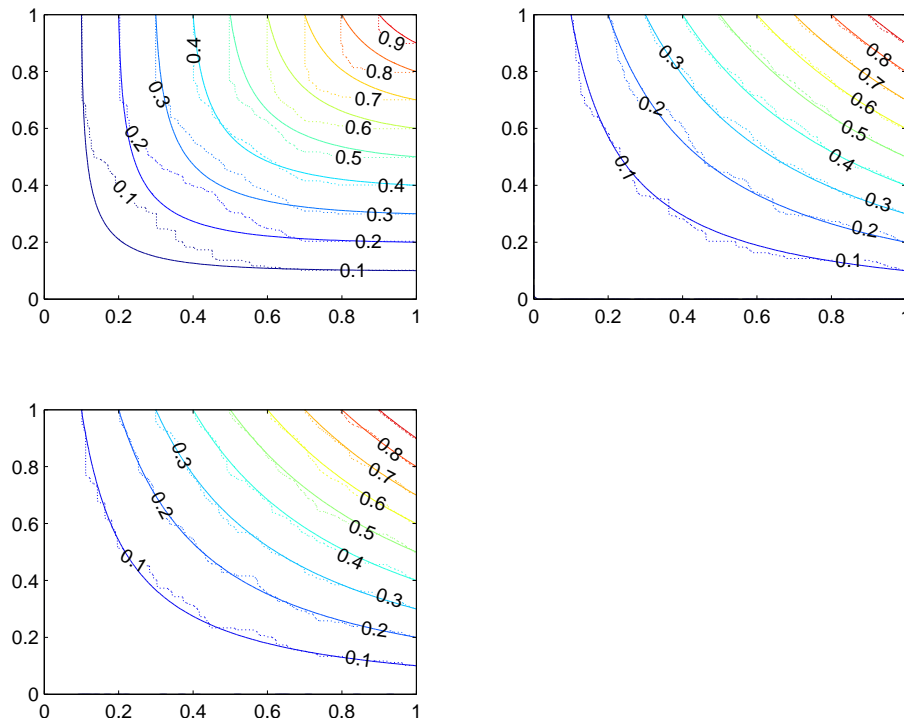


Figure 4. Contour plots of the empirical (dotted lines) and the fitted Frank copulas (solid lines) for the different trees in the three-dimensional vine copula for season 1. Bivariate copulas between W and V and V and D (top panel) and between $W|V$ and $D|V$ (bottom panel) are shown.

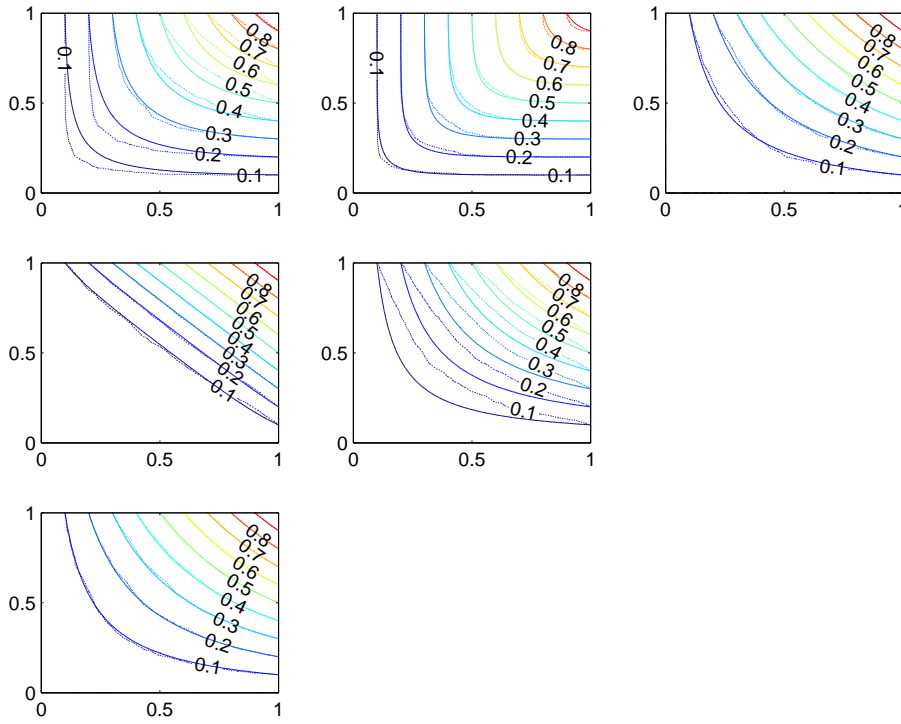


Figure 5. Contour plots of the empirical (dotted lines) and the fitted Frank copulas (solid lines) for the different trees in the four-dimensional vine copula for season 1. Bivariate copulas between p_d and W , W and V , and V and D (top panel), between $p_d|W$ and $V|W$, and $W|V$ and $D|V$ (middle panel) and between $p_d|WV$ and $D|WV$ (bottom panel) are shown.

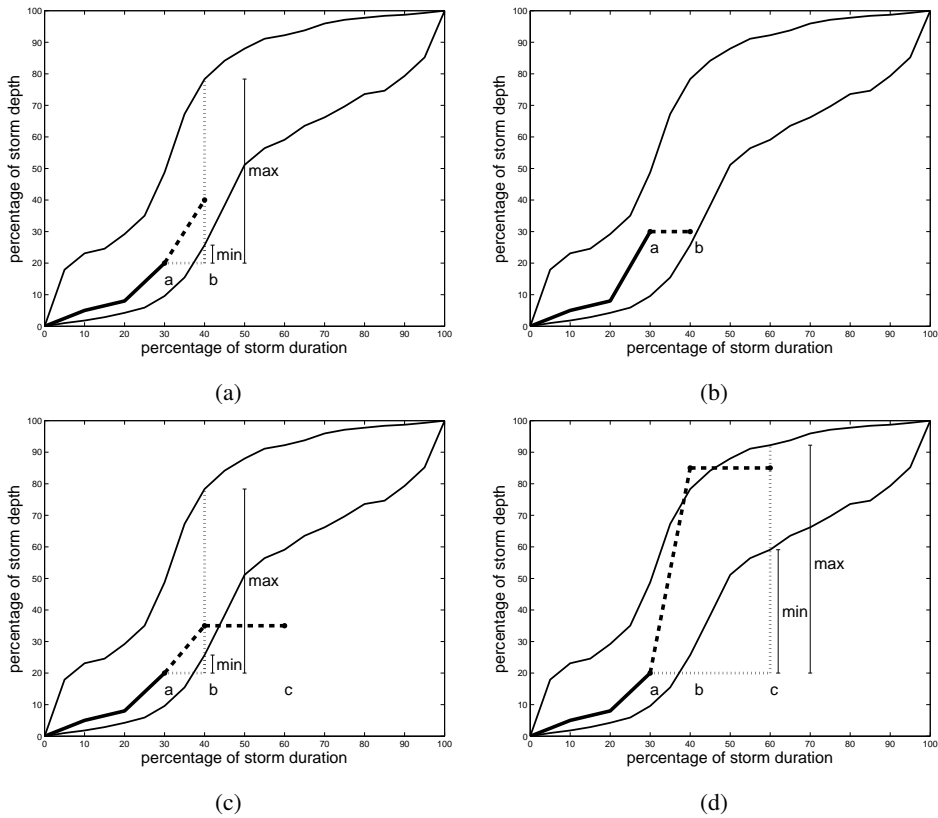


Figure 6. Illustration of the generation of an internal storm structure. **The part of the Huff curve that is already generated (up to time instant a) is indicated by a thick solid line. The value at time instant b needs to be determined. Four sampling strategies are possible:** Sampling in between two consecutive wet periods (case 1) (a), sampling at the end of a dry period (case 2) (b), sampling at the end of a wet period followed by a dry period with a selection on the basis of the current time **instant** (case 3) (c) and with a selection on the basis of the last time **instant** in the dry period (case 3) (d).

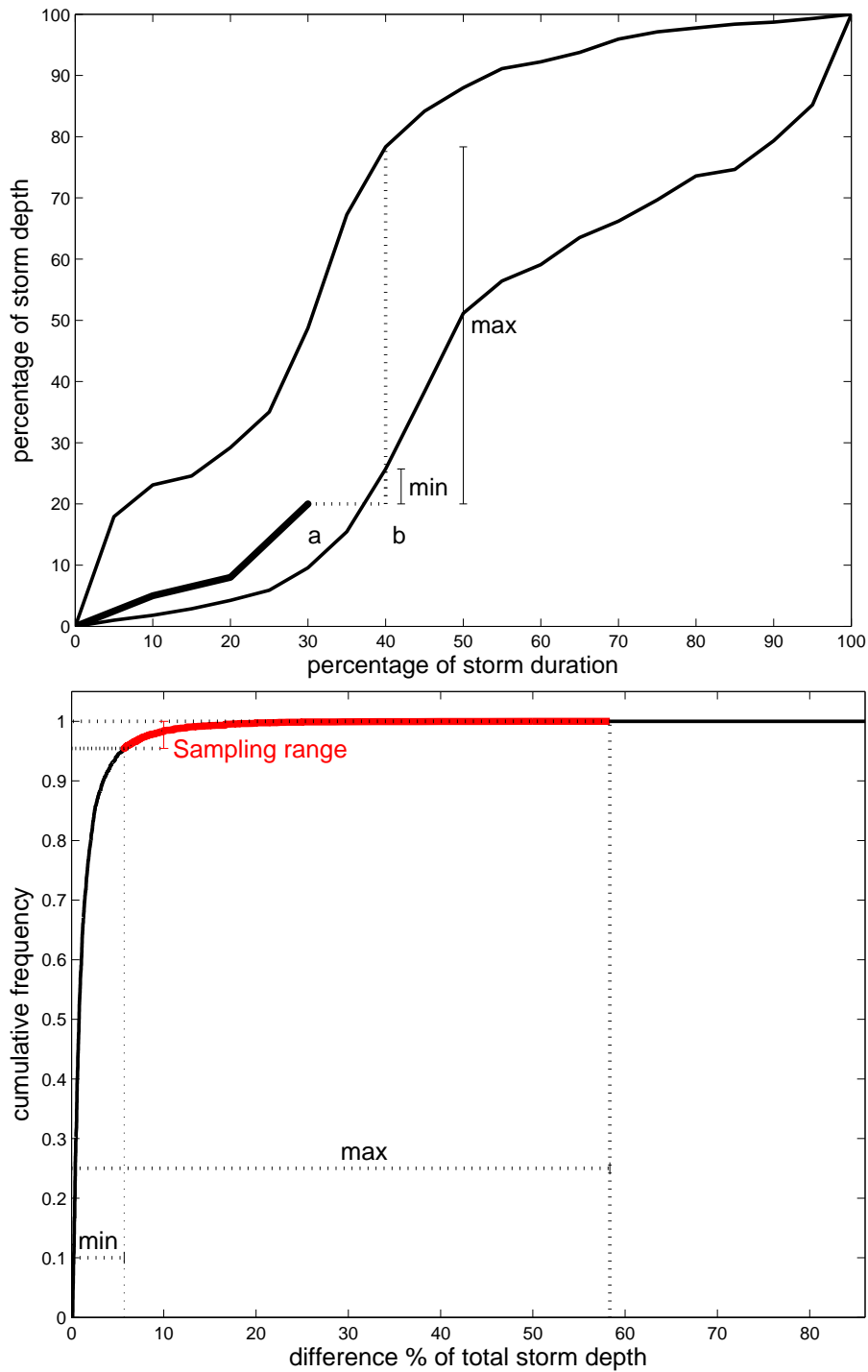
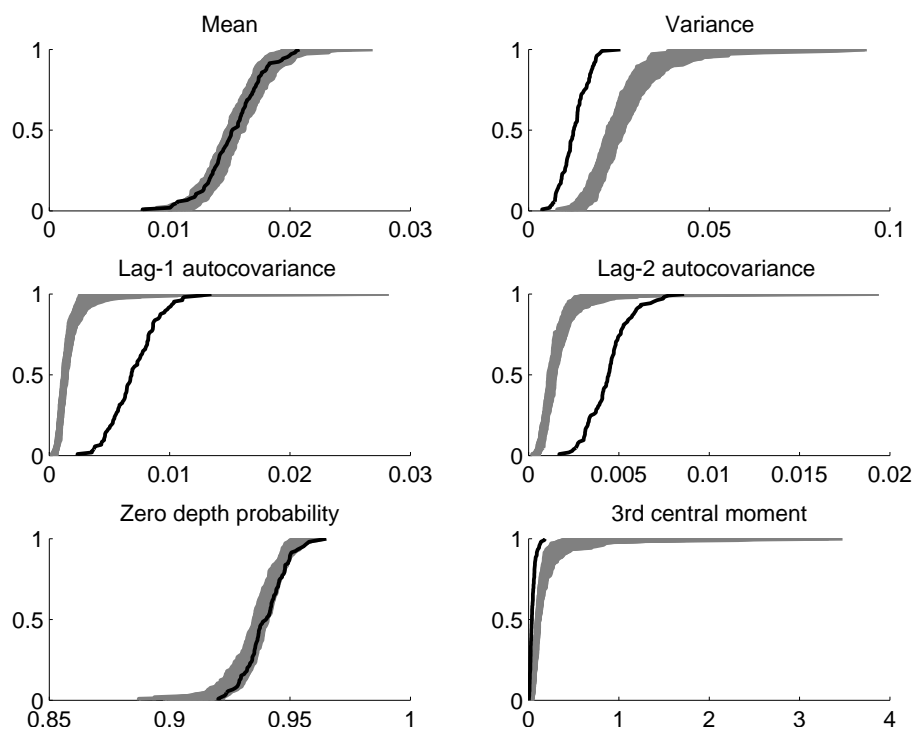
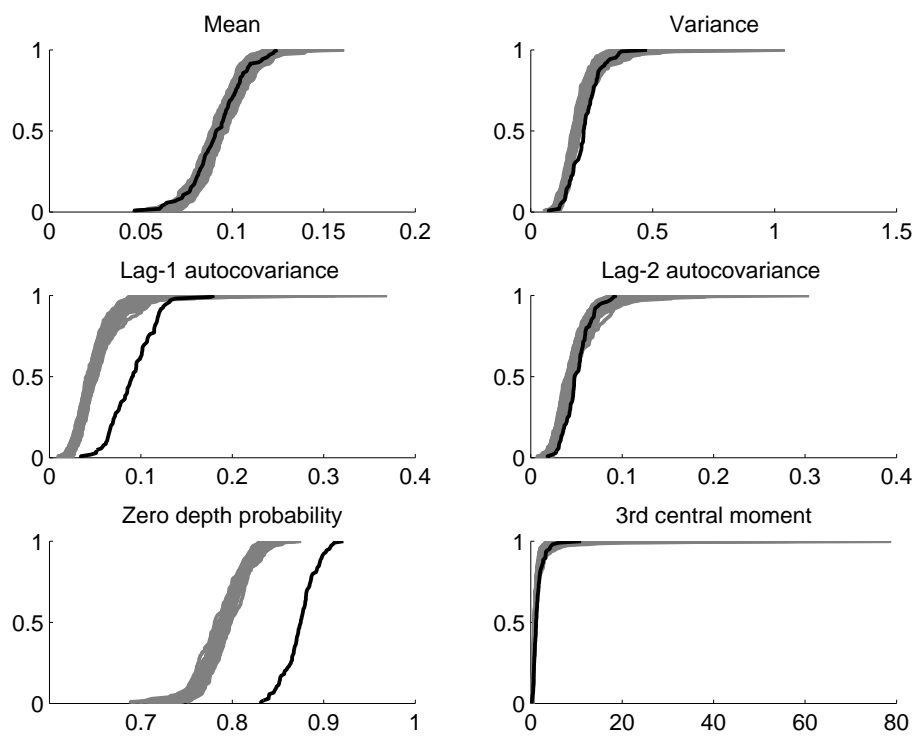


Figure 7. Illustration of the procedure to sample the storm depth at the next time instant (b). **First, the minimal and maximal increment in percentage of storm depth at time instant b are determined (top panel). Then, the corresponding sampling range in the cumulative distribution function of normalized increments is defined based on the minimal and maximal increment in percentage of storm depth derived from the top panel (bottom panel).**



(a)



(b)

Figure 8. Comparison of the empirical cumulative distributions of the yearly statistics of the observed time series (black line) and the bundle of empirical cumulative distributions of synthetic time series generated by means of the copula-based model (grey) at a 10-minute (a) and a 1-h aggregation level (b).

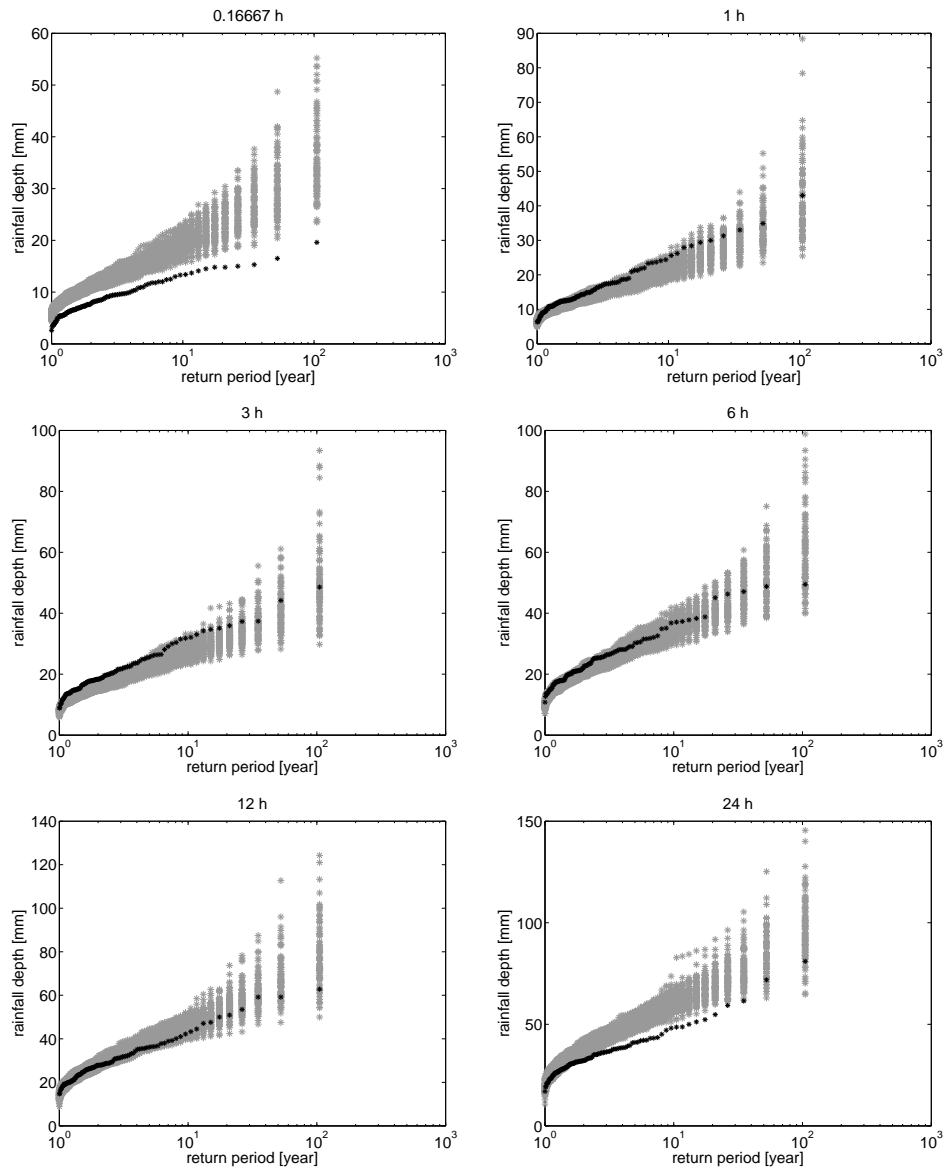


Figure 9. Comparison of empirically derived annual maxima related to the empirical return periods for different aggregation levels on the observed (black asterisks) and ensemble of synthetic time series generated by means of the copula-based rainfall model (grey asterisks).

Table 1. Observed probability of $p_d = 0$ for the storms in the different seasons

Probability of $p_d = 0$	
Winter	8.75%
Spring	11.21%
Summer	13.13%
Autumn	12.14%

Table 2. Correspondence between the observed and simulated pairwise dependences among (p_d, W, V, D) , expressed as Kendall's tau τ_K .

		observed 3D	observed 4D	simulated 3D	simulated 4D
season 1	τ_{12}	–	0.3040	–	0.3066
	τ_{23}	0.4140	0.6361	0.4118	0.6305
	τ_{34}	-0.0804	-0.0736	-0.0754	-0.0790
	τ_{13}	–	-0.0336	–	-0.0092
	τ_{24}	-0.0831	-0.0341	-0.0760	-0.0425
	τ_{14}	–	0.0259	–	0.0111
season 2	τ_{12}	–	0.3418	–	0.3423
	τ_{23}	0.5318	0.5888	0.5314	0.5866
	τ_{34}	-0.0773	-0.0778	-0.0811	-0.0649
	τ_{13}	–	-0.0183	–	-0.0018
	τ_{24}	-0.0397	-0.0410	-0.0421	-0.0416
	τ_{14}	–	0.0221	–	0.0026
season 3	τ_{12}	–	0.4060	–	0.4132
	τ_{23}	0.5243	0.5540	0.5248	0.5483
	τ_{34}	0.0247	-0.0855	0.0222	-0.0820
	τ_{13}	–	0.0411	–	0.0602
	τ_{24}	-0.0079	-0.0613	-0.0109	-0.0672
	τ_{14}	–	-0.0126	–	-0.0332
season 4	τ_{12}	–	0.3208	–	0.3276
	τ_{23}	0.4887	0.6058	0.4948	0.6016
	τ_{34}	-0.1066	-0.0779	-0.1084	-0.0816
	τ_{13}	–	-0.0287	–	-0.0080
	τ_{24}	-0.1377	-0.0636	-0.1680	-0.0737
	τ_{14}	–	-0.0086	–	-0.0099

Table 3. Parameters of the bivariate Frank copulas in the construction of the three- and four-dimensional vine copulas.

	parameter	(W, V, D)	(p_d, W, V, D)
season 1	θ_{12}	–	2.9632
	θ_{23}	4.3567	8.9789
	θ_{34}	-0.7276	-0.6651
	$\theta_{13 2}$	–	-9.1797
	$\theta_{24 3}$	-0.4077	0.4199
	$\theta_{14 23}$	–	-0.4670
season 2	θ_{12}	–	3.4077
	θ_{23}	6.3457	7.6379
	θ_{34}	-0.6992	-0.7037
	$\theta_{13 2}$	–	-7.6601
	$\theta_{24 3}$	0.2150	0.2348
	$\theta_{14 23}$	–	-0.2741
season 3	θ_{12}	–	4.2445
	θ_{23}	6.1971	6.8144
	θ_{34}	0.2221	-0.7737
	$\theta_{13 2}$	–	-6.0083
	$\theta_{24 3}$	-0.3429	0.0194
	$\theta_{14 23}$	–	-0.2419
season 4	θ_{12}	–	3.1574
	θ_{23}	5.5352	8.0877
	θ_{34}	-0.9686	-0.7041
	$\theta_{13 2}$	–	-8.1955
	$\theta_{24 3}$	-1.1409	-0.0918
	$\theta_{14 23}$	–	-0.0958

Table 4. Probability of a storm to belong to a certain quartile group.

quartile group	probability [-]
first	0.3930
second	0.2063
third	0.1826
fourth	0.2181